

On the degeneracy between $f\sigma_8$ tension and its Gaussian process forecasting

Mauricio Reyes*

Institute of Physics, Laboratory of Astrophysics, EPFL, 1290 Versoix, Switzerland.

Celia Escamilla-Rivera†

*Instituto de Ciencias Nucleares, Universidad Nacional Autónoma de México,
Circuito Exterior C.U., A.P. 70-543, México D.F. 04510, México.*

In this paper we reconstruct the growth and evolution of the cosmic structure of the Universe using Markov Chain Monte Carlo algorithms for Gaussian processes [1]. We estimate the difference between the reconstructions that are calculated through a maximization of the kernel hyperparameters and those that are obtained with a complete exploration of the parameter space. We find that the difference between these two approaches is of the order of 1%. Furthermore, we compare our results with those obtained by Planck Collaboration 2018 assuming a Λ CDM model and we do not find a statistically significant difference in the redshift range where the reconstructions of $f\sigma_8$ have been made.

I. INTRODUCTION

Currently, the estimates of the value of $S_8 \equiv \sigma_8 \sqrt{\Omega_m}/0.3$, obtained from the Λ CDM fit to the Cosmic Microwave Background (CMB) differ between 2-3 σ with respect to the value of S_8 obtained with the analysis of galaxy clustering using two-point correlation functions (2PCFs) [2]. This discrepancy is the so-called S_8 tension [3, 4]. Additionally, the most recent estimate of the value of the Hubble constant, H_0 , obtained with the calibration of the cosmic distance ladder scale through Cepheid stars and supernovae type Ia is 5σ different [5] from the value Λ CDM obtained with CMB observations.

In specific, the primary anisotropies of the CMB exhibit a tension in the matter clustering strength at the level of 2 – 3 σ when compared to lower z probes such as weak gravitational lensing and galaxy clustering (e.g. [2, 6–14]). The lower z probes (see Figure 4 from [15]), select a lower value of S_8 compared to the high z CMB estimates. The measured S_8 value is model dependent and in the majority of the scenarios it is considered a standard flat Λ CDM model. Of course, this latter model provides a well fit to the data from all probes, but predicts a lower value of structure formation compared to what we expect from the CMB [7]. In [15] it is reported latter parameter estimates and constraints, where we notice that there might be slightly differences in the selection that enter each studies. For example, on one hand a statistical property of the S_8 distribution might be selected, such as its mean or mode together with the asymmetric 68% C.L around this value or the standard deviation of the data points. On the other hand, the statistics to the full posterior distribution can be adopted, such as the maximum a posteriori point or the best fitting values and its errors. Anyhow, these considerations can affect the estimated values of

the parameters, in particular when the posterior distributions are significantly non-Gaussian.

Many beyond Λ CDM models have been proposed as tentative explanations to this observed S_8 tension, however non specific model has been proven much better than the standard one. In such case, we should look for a reason in where the tension between CMB and cosmic shear in the inferred value of S_8 can arise from unaccounted baryonic physics, other unknown systematics or a statistical fluke. Furthermore, we require that S_8 can be independent of CMB and cosmic shear. In this matter, redshift-space distortion (RSD) data also prefer a small value of S_8 that is 2-3 σ lower than the Planck result [16]. However, the RSD values on S_8 is sensitive to the cosmological model.

In this *paper* we perform the reconstructions of the $f\sigma_8(z)$ observations using Gaussian processes (GP) to analyze if the reconstructions suggest possible deviations with respect to the standard cosmological model. Unlike previous studies [17–19], we take into account the Planck 2018 confidence contours when comparing the predictions of Λ CDM with those of the reconstructions. This allows to keep in control the statistical uncertainties. The possibility of using GP to distinguish between Modified Gravity (MG) and General Relativity (GR) has been analyzed [20], e.g. treating the perturbations of a disformally scalar field model which background mimics the Λ CDM [21].

Previous articles [18] have used the reconstructions of the Hubble parameter to reconstruct $f\sigma_8(z)$ and to show how different values of H_0 change the value of the $f\sigma_8$ tension. However, the large number of free parameters associated with that approach leads to large uncertainties on the reconstructions, which could explain why a $\sim 4\sigma$ change in the value of H_0 only causes a $\sim 1\sigma$ change on the value of the $f\sigma_8$ tension.

Unlike the standard way to reconstruct $f\sigma_8$ [18], in this work we reconstruct $f\sigma_8(z)$ using directly the estimations of $f\sigma_8$, therefore it will be possible to remove H_0 and σ_8 as free parameters and reduce the uncertainty in the confidence contours. However, we should mention that

*Electronic address: mauricio.cruzreyes@epfl.ch

†Electronic address: celia.escamilla@nucleares.unam.mx

our approach does not allow us to obtain a direct estimate of the aforementioned parameters.

In this line of thought, several numerical methods have been developing upon these years, showing a great advance in the precision cosmology road, e.g. methods that involves artificial neural network (ANN) to reconstruct late-time cosmology data [22], creation of mock datasets through machine learning (ML) based on the LSST survey and using a fiducial cosmology [23] and bayesian analyses in order to re-assessed the σ_8 discrepancy between CMB and weak lensing data [16].

Furthermore, we analyse two different approaches to obtain the value of the confidence contours of the reconstructions. The first approach consists on the maximization of the likelihood associated with the GP in order to obtain the value of the free parameters from the reconstruction. This approach has been frequently used in the literature to perform GP in the context of cosmology [18, 20, 24–26], however in some works [27, 28] it has been shown that this process could lead to an underestimation of the confidence contours of the reconstructions. The second approach consists in an exploration of the parameter space of the free parameters through Markov Chains Monte Carlo (MCMC) methods. This method allows us to obtain an estimate of the uncertainties associated with each parameter, which contributes to solve the underestimation problem.

II. TREATMENT OF DATA SAMPLES AND METHODOLOGY

To use GP method, we need to assume that our set of observations “ \mathbf{y} ” given in the set of redshifts “ \mathbf{z} ” is Gaussian distributed around the underlying function that we seek to reconstruct, $\mathbf{g}(\mathbf{z})$. This allows us to associate a probability distribution with the data:

$$\mathbf{y} \sim \mathcal{N}(\bar{\mu}, K(\mathbf{z}, \mathbf{z}) + C), \quad (1)$$

where $\bar{\mu}$ is the mean value of the observations, C is its covariance matrix and K is the covariance matrix associated with the Gaussian processes also known as kernel function. It can be shown that the mean value and covariance matrix of the reconstructed function in the set of redshifts \mathbf{z}^* is given by [27]

$$\bar{g} = \bar{\mu}^* + K(\mathbf{z}^*, \mathbf{z}) [K(\mathbf{z}, \mathbf{z}) + C]^{-1} (y - \bar{\mu}), \quad (2)$$

$$C(g^*) = K(\mathbf{z}^*, \mathbf{z}^*) - K(\mathbf{z}^*, \mathbf{z}) [K(\mathbf{z}, \mathbf{z}) + C]^{-1} K(\mathbf{z}, \mathbf{z}^*). \quad (3)$$

Measurements of the clustering pattern of matter in the redshift space allows us to infer parameters such as the linear growth of matter perturbations $f(z)$ and the variance of matter fluctuations σ_R^2 on a given scale R . Variance is usually reported on a scale $R = 8h^{-1}$ Mpc, that is, σ_8^2 .

However, an exact determination of the value of $f(z)$ turns out to be complex, since the galaxy redshift surveys provide an estimate of the perturbations in terms of

galaxy densities δ_g instead not directly in terms of matter density $\delta_g = b\delta_m$. Unfortunately, the exact value of the parameter b remains uncertain [29], for that reason, the measurements are reported in terms of $f\sigma_8(z)$ since it is independent of the parameter b [18].

To perform the reconstructions we use the compilation of measurements of $f\sigma_8(z)$ shown in Table I of [30]. This table contains 30 measurements of $f\sigma_8$, together with their uncertainties and their covariance matrices.

According to the latter, the inferred values of $f\sigma_8(z)$ depend on two things: (i) the anisotropies in the power spectrum of peculiar velocities of galaxies and (ii) the fiducial cosmology chosen to estimate the values of $f\sigma_8(z)$. If the cosmology chosen to perform the data analysis does not adequately describe the geometry of the universe, then nontrivial anisotropies are introduced in the 2PCFs, which are directly correlated with the estimated value of $f\sigma_8$, this effect is known as Alcock-Paczynski (AP) effect. Is important to that the $f\sigma_8(z)$ values sometimes are reported assuming [31] different fiducial cosmologies, e.g.

- When considering a fiducial cosmology with $\Omega_m^0 = 0.26479$, $H_0 = 71$ km/s/Mpc, $\sigma_8 = 0.8$, $z_{\text{eff}} = 1.52$, it is obtained $f\sigma_8(z_{\text{eff}}) = 0.420 \pm 0.076$ [32].
- While with a fiducial cosmology with $\Omega_m^0 = 0.31$, $H_0 = 67.6$ km/s/Mpc, $\sigma_8 = 0.8225$, $z_{\text{eff}} = 1.52$, we can obtain $f\sigma_8(z_{\text{eff}}) = 0.396 \pm 0.079$ [33].

III. ALCOCK-PACZYNSKI CORRECTIONS

If the $f\sigma_8(z)$ reconstructions are performed without including corrections to the AP effect, then all the information from different fiducial cosmologies would be mixed, i.e it cannot be possible to properly estimate the tension between the reconstructions and the Λ CDM model. We apply the correction to the AP effect given in [31], whose corrections state that if a measurement of $f\sigma_8(z)$ has been obtained assuming a fiducial cosmology with a Hubble parameter $\bar{H}(z)$ and angular diameter $\bar{D}_A(z)$, then the corresponding value of $f\sigma_8(z)$ assuming a different fiducial cosmology with $H(z)$ and $\bar{D}_a(z)$ can be approximated as:

$$f\sigma_8(z) \approx \frac{H(z)D_A(z)}{\bar{H}(z)\bar{D}_A(z)} \bar{f}\sigma_8(z). \quad (4)$$

To correct the AP effect, we consider a *vanilla* Λ CDM cosmology with the parameters inferred from Planck 2018 Collaboration [34], such as the high redshift data from Planck TT,TE,EE+lowE is $S_8 = 0.834 \pm 0.016$. Combining this data with secondary CMB anisotropies, in the form of CMB lensing, serves to tighten the constraint to $S_8 = 0.832 \pm 0.013$.

To proceed with this calculation, we set the following steps:

1. Suppose that $A(z_i)$ and $B(z_j)$ are two measurements of $f\sigma_8(z)$ that were obtained assuming the

fiducial cosmology $H(z)$

$$A(z_i) = \mu_a \pm \sigma_a, \quad (5)$$

$$B(z_j) = \mu_b \pm \sigma_b, \quad (6)$$

with μ_a, μ_b the mean value of each measurement and σ_a, σ_b their 1σ uncertainties, also suppose that the measurements are correlated through a covariance matrix C

$$C = \begin{pmatrix} \sigma_a^2 & \sigma_{ab} \\ \sigma_{ba} & \sigma_b^2 \end{pmatrix}. \quad (7)$$

2. In order to compute the value of $A(z_i)$ and $B(z_j)$ in a fiducial cosmology $H'(z)$, we have to perform the AP correction. To do so, we multiply A and B with constants C_A and C_B given by the equation (4) and then the covariance matrix for AC_a and BC_b , is given by [35]

$$C' = \begin{pmatrix} (C_a\sigma_a)^2 & C_aC_b\sigma_{ab} \\ C_aC_b\sigma_{ba} & (C_b\sigma_b)^2 \end{pmatrix}. \quad (8)$$

IV. KERNEL METRICS

It has been shown that the kernel chosen to perform the reconstructions can affect the uncertainties of the parameters derived from the reconstructions [27, 28, 36]. In particular, the Gaussian kernel can lead to uncertainties up to three times smaller than the value of the uncertainties obtained with the Matérn covariance functions [37], since this could be associated with the problem of underestimation of uncertainties, we choose to use only Matérn kernels, specifically the Matérn 3/2 and Matérn 5/2 kernels. These covariance functions have been used, e.g. in studies that analyze how the choice between different kernels affect the value of H_0 that is obtained from the reconstructions of the cosmic late expansion [36] and in analysis on how different kernels can affect the constraints on modified theories of gravity [24]. The Matérn 3/2 and Matérn 5/2 kernels are respectively defined as:

$$\mathbf{K}_{ij} = \eta^2 \left(1 + \frac{\sqrt{3}(z_i - z_j)^2}{l} \right) \exp \left(-\frac{\sqrt{3}(z_i - z_j)^2}{l} \right) \rightarrow \text{Matérn 3/2}, \quad (9)$$

$$\mathbf{K}_{ij} = \eta^2 \left(1 + \frac{\sqrt{5}(z_i - z_j)^2}{l} + \frac{5(z_i - z_j)^2}{3l^2} \right) \exp \left(-\frac{\sqrt{5}(z_i - z_j)^2}{l} \right) \rightarrow \text{Matérn 5/2}, \quad (10)$$

where η and l are free parameters that measure the width of the reconstructed function and the correlation between the function evaluated at two given points z_i and z_j . With these kernels at hand we are ready to proceed with two different methods to obtain the value of the hyperparameters of the kernel:

- *Method (i)* consists on the maximization of the likelihood associated with the observations Eq. (1).
- *Method (ii)* consists in a full exploration of parameter space for the hyperparameters through MCMC methods. This approach is convenient when the parameter space is multidimensional and it could help us to find the true maximum likelihood estimate in cases were the algorithm for maximization gets stuck in a local minima.

Since η is a squared quantity in both covariance functions (9)-(10), if $(\eta_{\text{Max}}, l_{\text{Max}})$ are the values of the hyperparameters that maximize Eq.(1), then $(-\eta_{\text{Max}}, l_{\text{Max}})$ also maximize Eq.(1), this leads to a bimodal posterior distribution for the hyperparameter η^M . Since with one mode we can obtain the full information to carry out the reconstructions, it is convenient to establish priors that only take into account the positive (or negative) branch of the parameter space for η . With this method it is possible to reduce the computational time required to

calculate the posterior distribution of the hyperparameters and also it allow us to avoid convergence problems within the numerical code.

Notice that the covariance functions (9) and (10) are not symmetric on l . However, we expect positive values of l , otherwise the correlation between the points z_i, z_j will grow proportionally to

$$\mathbf{K}_{ij} \propto \exp \left(-\frac{|z_i - z_j|}{l} \right). \quad (11)$$

Since hyperparameters are restricted to be positive, we consider for them Gamma probability distributions as priors. The probability density function $P(X)$ for a random variable X that follows a Gamma distribution with parameters α and β , is given by

$$P(X) = \begin{cases} 0 & \text{if } X \leq 0, \\ \frac{\beta(\beta X)^{\alpha-1} e^{-\beta X}}{\Gamma(\alpha)} & \text{if } X > 0, \end{cases} \quad (12)$$

with Γ the Gamma function. The mean value of the $P(X)$ is $M = \alpha/\beta$, the mode is $M_0 = (\alpha - 1)/\beta$ and the variance is $\text{Var}(X^2) = \alpha/\beta^2$ [35]. In order to find the value of the hyperparameters of the covariance functions that maximizes Eq.(1) we perform a Maximum Likelihood Estimation (MLS) with the code [27], and afterwards we proceed with a standard MCMC analysis using the public available code PyMC3 [38]. For both hyperparameters we choose Gamma priors with $\beta = 1$ and α

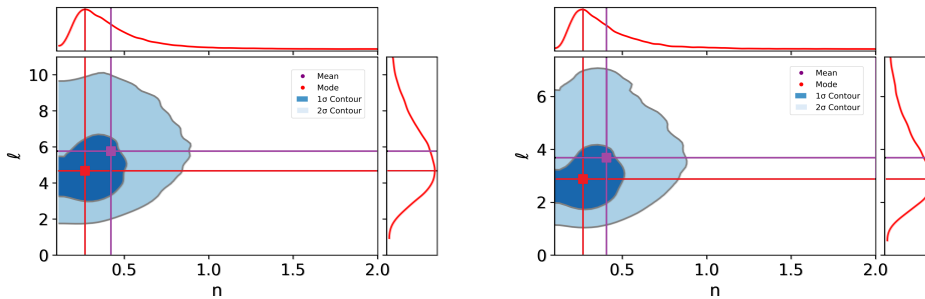


Figure 1: *Left*: 1σ and 2σ confidence contours for the hyperparameters of the Matérn 3/2 kernel (9). *Right*: 1σ and 2σ confidence contours for the hyperparameters of the Matérn 5/2 kernel (10). The posterior that appear on top and right side show the marginal distributions for each hyperparameter. The purple and red color dots show the region of parameter space where the mean (purple) and mode (red) of each hyperparameter intersects.

equal to their MLS. We estimate the convergence of the chains using a Gelman-Rubin convergence criteria [39] with $R - 1 < 0.03$. The reconstructions are estimated with two different approaches: (1) we use the mean value of the hyperparameters to estimate the mean value of the reconstructions and (2) we use the mode. Our results are detailed in Tables I-II and in Figure 2.

In order to distinguish between reconstructions we define the tension metric as follows:

$$T(z) = \frac{|f\sigma_8^{rec}(z) - f\sigma_8^{\Lambda\text{CDM}}(z)|}{\sqrt{\sigma_{rec}^2(z) + \sigma_{\Lambda\text{CDM}}^2(z)}}, \quad (13)$$

where $f\sigma_8^{rec}(z)$, $f\sigma_8^{\Lambda\text{CDM}}(z)$ are the mean values of the reconstructions and ΛCDM , respectively. $\sigma_{rec}(z)$, $\sigma_{\Lambda\text{CDM}}(z)$ are the 1σ statistical uncertainties. Notice that Eq.(13) quantifies the difference in standard deviations between the reconstructions and ΛCDM .

From Tables III and IV we can notice that for both kernels the tension for all methods is of the order of 2σ in the observable redshift region. The mean value of the reconstructions obtained through the different methods represent 1% of its total value.

Additionally, to test the performance of each model describing by the observations, we estimate the chi-square statistics as follows

$$\Delta f\sigma_8|_i = f\sigma_{8,obs}(z_i) - f\sigma_{8,recons}(z_i), \quad (14)$$

$$\chi^2 = \Delta f\sigma_8^T \cdot C^{-1} \cdot \Delta f\sigma_8, \quad (15)$$

with C^{-1} the inverse of the covariance matrix of the data. The results are shown in Tables V and VI, with these results and with those obtained using the $T(z)$ function, we conclude that there is no statistical significant difference

between ΛCDM and the reconstructions presented here (see Tables V and VI).

V. CONCLUSIONS

In this paper we reconstructed the $f\sigma_8$ observations using two different kernels and three different methods to obtain the value of the hyperparameters. The tension between ΛCDM and the reconstructions does not give values above 2.2σ . We showed that choosing different kernels leads to differences of the order of $\sim 0.1\sigma$ in the value of the tension. Furthermore, we also show that the change in the value of the tension obtained with different methods (with the kernel fixed) is also of the order of 0.1σ . Therefore, we conclude that there is not significant statistical difference between the predictions given for $f\sigma_8(z)$ by ΛCDM with Planck 2018 parameters and those given by the reconstructions, since the maximum tension between both is below 2.2σ .

Acknowledgments. - MC acknowledge support from the European Research Council (ERC) under the European Union's Horizon 2020 research and innovation programme (Grant Agreement No. 947660). CE-R is supported by DGAPA-PAPIIT UNAM Project TA100122 and acknowledges the Royal Astronomical Society as FRAS 10147. This work is part of the Cosmostatistics National Group (CosmoNag) project. The Authors would like to acknowledge the PyMC3 and Arviz communities for their helpful recommendations on the modified version of arviz code [40].

-
- [1] Michalis K Titsias, Neil Lawrence, and Magnus Rattray. Markov chain Monte Carlo algorithms for Gaussian processes. *Inference and Estimation in Probabilistic Time-Series Models*, 9:298, 2008.
- [2] T. M. C. Abbott et al. Dark Energy Survey Year 3 re-

- sults: Cosmological constraints from galaxy clustering and weak lensing. *Phys. Rev. D*, 105(2):023520, 2022.
- [3] Tilman Tröster et al. Cosmology from large-scale structure: Constraining ΛCDM with BOSS. *Astron. Astrophys.*, 633:L10, 2020.

Parameter	MLS	Mean value	Standard deviation	Mode
l	5.36	5.73	2.25	4.50
η	0.33	0.42	0.24	0.26

Table I: Hyperparameters statistics summary for the Matérn 3/2 kernel (9). *First column:* indicates the kernel hyperparameters. *Second column:* denotes the value Maximum Likelihood Estimation (MLS) for the hyperparameters. *Third column:* shows the mean value of the posterior distribution for each hyperparameter obtained using a MCMC. *Fourth column:* shows the standard deviation. *Fifth column:* indicates the mode.

Parameter	MLS	Mean value	Standard deviation	Mode
l	3.33	3.71	1.70	2.80
η	0.32	0.41	0.26	0.27

Table II: Hyperparameters statistics summary for the Matérn 5/2 kernel (10). The meaning of columns is the same as in Table I.

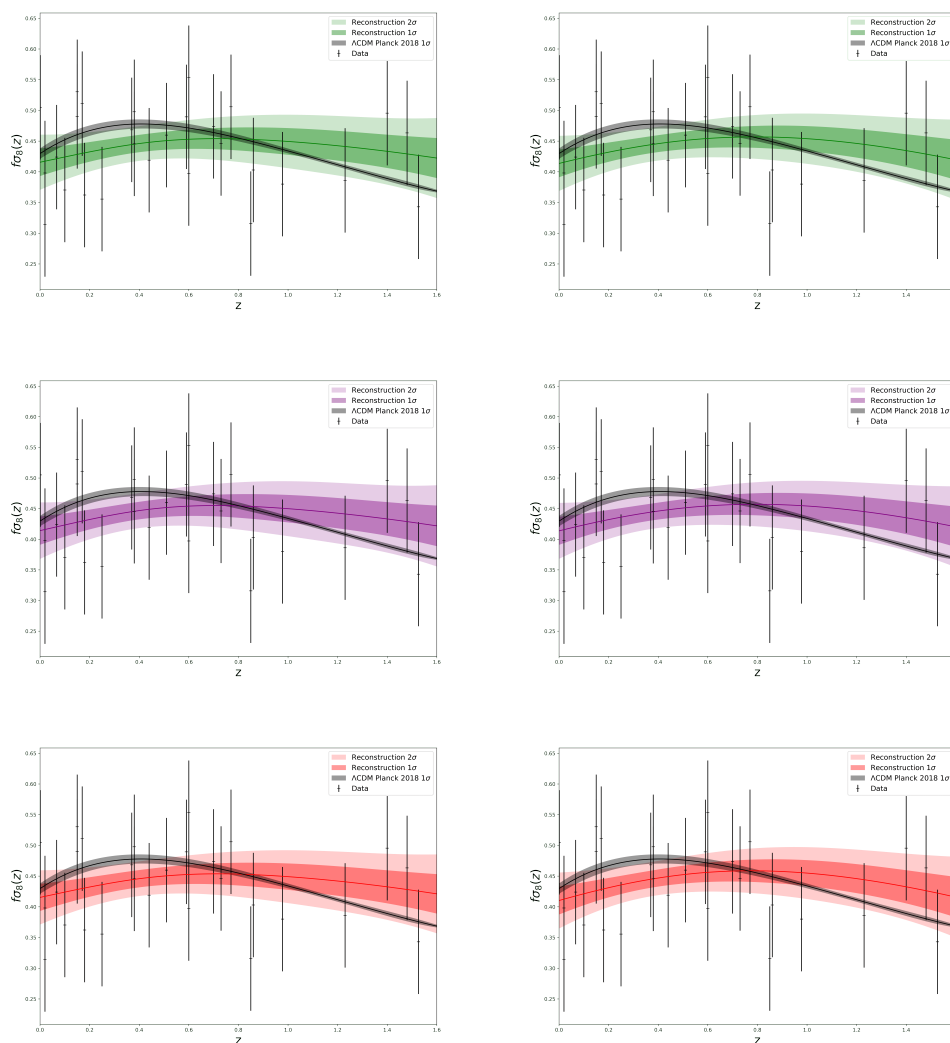


Figure 2: *Left:* Reconstructions of $f\sigma_8(z)$ with the Matérn 3/2 kernel (9). *Right:* Reconstructions of $f\sigma_8(z)$ with the Matérn 5/2 kernel (9). *Top:* Reconstructions obtained using the Maximum likelihood method (green color). *Middle:* Reconstructions obtained using the mean value of the hyperparameters (purple color). *Bottom:* Reconstructions obtained using the mode of the hyperparameters (red color). The data is denoted by the black points. In gray we shown the prediction for $f\sigma_8(z)$ given a fitted Λ CDM with CMB Planck 2018 values [34]. Confidence contours of each reconstruction are shown at 1σ and 2σ level.

Method	Redshift of maximum difference	Maximum difference	Total difference
Mean	0.30	2.09	1.95
Mode	0.31	2.15	2.00
MLS	0.31	2.13	1.99

Table III: Comparison between the different methods analyzed in this work and Λ CDM. First column shows the method used to estimate the value of the hyperparameters of the Matérn 3/2 kernel. Second column shows the redshift where Eq. (13) reach his maximum, third column shows the value of $T(z)$ reached at that redshift and the fourth shows the result of integrating $T(z)$ in the redshift range were the reconstructions were performed.

Method	Redshift of maximum difference	Maximum difference	Total difference
Mean	0.3	2.18	2.12
Mode	0.3	2.17	2.06
MLS	0.3	2.19	2.12

Table IV: Comparison between the different methods analyzed in this work and Λ CDM. The description by columns are the same as the ones reported in Table III but for the Matérn 5/2 kernel.

Method	χ^2
Λ CDM	0.85
Mean	0.77
Mode	0.78
MLS	0.77

Table V: χ^2 -statistics over the number of degrees of freedom ($N = 28$) for Λ CDM and the different reconstructions obtained using the kernel Matérn 3/2.

Method	χ^2
Mean	0.78
Mode	0.77
MLS	0.78

Table VI: χ^2 -statistics over the number of degrees of freedom ($N = 28$) for the different reconstructions obtained using the kernel Matérn 5/2.

- [4] Eleonora Di Valentino et al. Cosmology Intertwined III: $f\sigma_8$ and S_8 . *Astropart. Phys.*, 131:102604, 2021.
- [5] Adam G Riess, Wenlong Yuan, Lucas M Macri, Dan Scolnic, Dillon Brout, Stefano Casertano, David O Jones, Yukei Murakami, Louise Breuval, Thomas G Brink, et al. A Comprehensive Measurement of the Local Value of the Hubble Constant with 1 km/s/Mpc Uncertainty from the Hubble Space Telescope and the SH0ES Team. *arXiv preprint arXiv:2112.04510*, 2021.
- [6] Marika Asgari et al. KiDS+VIKING-450 and DES-Y1 combined: Mitigating baryon feedback uncertainty with COSEBIs. *Astron. Astrophys.*, 634:A127, 2020.
- [7] Marika Asgari et al. KiDS-1000 Cosmology: Cosmic shear constraints and comparison between two point statistics. *Astron. Astrophys.*, 645:A104, 2021.
- [8] S. Joudaki et al. KiDS+VIKING-450 and DES-Y1 combined: Cosmology with cosmic shear. *Astron. Astrophys.*, 638:L1, 2020.
- [9] A. Amon et al. Dark Energy Survey Year 3 results: Cosmology from cosmic shear and robustness to data calibration. *Phys. Rev. D*, 105(2):023514, 2022.
- [10] L. F. Secco et al. Dark Energy Survey Year 3 results: Cosmology from cosmic shear and robustness to modeling uncertainty. *Phys. Rev. D*, 105(2):023515, 2022.
- [11] A. Loureiro et al. KiDS & Euclid: Cosmological implications of a pseudo angular power spectrum analysis of KiDS-1000 cosmic shear tomography. 10 2021.
- [12] H. Hildebrandt et al. KiDS+VIKING-450: Cosmic shear tomography with optical and infrared data. *Astron. Astrophys.*, 633:A69, 2020.
- [13] T. M. C. Abbott et al. Dark Energy Survey Year 1 Results: Cosmological constraints from cluster abundances and weak lensing. *Phys. Rev. D*, 102(2):023509, 2020.
- [14] Oliver H. E. Philcox and Mikhail M. Ivanov. BOSS DR12 full-shape cosmology: Λ CDM constraints from the large-scale galaxy power spectrum and bispectrum monopole. *Phys. Rev. D*, 105(4):043517, 2022.
- [15] Elcio Abdalla et al. Cosmology intertwined: A review of the particle physics, astrophysics, and cosmology associated with the cosmological tensions and anomalies. *JHEAp*, 34:49–211, 2022.
- [16] Rafael C. Nunes and Sunny Vagnozzi. Arbitrating the S_8 discrepancy with growth rate measurements from redshift-space distortions. *Mon. Not. Roy. Astron. Soc.*, 505(4):5427–5437, 2021.
- [17] David Benisty. Quantifying the S_8 tension with the Redshift Space Distortion data set. *Phys. Dark Univ.*, 31:100766, 2021.

- [18] En-Kun Li, Minghui Du, Zhi-Huan Zhou, Hongchao Zhang, and Lixin Xu. Testing the effect of H_0 on $f\sigma_8$ tension using a Gaussian process method. *Mon. Not. Roy. Astron. Soc.*, 501(3):4452–4463, 2021.
- [19] Jackson Levi Said, Jurgen Mifsud, Joseph Sultana, and Kristian Zarb Adami. Reconstructing teleparallel gravity with cosmic structure growth and expansion rate data. *JCAP*, 06:015, 2021.
- [20] Mauricio Reyes and Celia Escamilla-Rivera. Improving data-driven model-independent reconstructions and updated constraints on dark energy models from Horndeski cosmology. *JCAP*, 07:048, 2021.
- [21] Avishek Dusoye, Alvaro de la Cruz-Dombriz, Peter Dunsby, and Nelson J. Nunes. Constraining disformal couplings with Redshift Space Distortion. 12 2021.
- [22] Konstantinos Dialektopoulos, Jackson Levi Said, Jurgen Mifsud, Joseph Sultana, and Kristian Zarb Adami. Neural network reconstruction of late-time cosmology and null tests. *Journal of Cosmology and Astroparticle Physics*, 2022(02):023, 2022.
- [23] Rubén Arjona, Alessandro Melchiorri, and Savvas Nesseris. Testing the Λ CDM paradigm with growth rate data and machine learning. 7 2021.
- [24] Rebecca Briffa, Salvatore Capozziello, Jackson Levi Said, Jurgen Mifsud, and Emmanuel N. Saridakis. Constraining teleparallel gravity through Gaussian processes. *Class. Quant. Grav.*, 38(5):055007, 2020.
- [25] Louis Perenon, Matteo Martinelli, Stéphane Ilić, Roy Maartens, Michelle Lochner, and Chris Clarkson. Multi-tasking the growth of cosmological structures. *Phys. Dark Univ.*, 34:100898, 2021.
- [26] Jaime Ruiz-Zapatero, Carlos García-García, David Alonso, Pedro G. Ferreira, and Richard D. P. Grumitt. Model-independent constraints on Ω_m and $H(z)$ from the link between geometry and growth. 1 2022.
- [27] Marina Seikel, Chris Clarkson, and Mathew Smith. Reconstruction of dark energy and expansion dynamics using gaussian processes. *Journal of Cosmology and Astroparticle Physics*, 2012(06):036, 2012.
- [28] Celia Escamilla-Rivera, Jackson Levi Said, and Jurgen Mifsud. Performance of Non-Parametric Reconstruction Techniques in the Late-Time Universe. 5 2021.
- [29] Savvas Nesseris, George Pantazis, and Leandros Perivolaropoulos. Tension and constraints on modified gravity parametrizations of $G_{\text{eff}}(z)$ from growth rate and Planck data. *Physical Review D*, 96(2):023542, 2017.
- [30] Louis Perenon, Julien Bel, Roy Maartens, and Alvaro de la Cruz-Dombriz. Optimising growth of structure constraints on modified gravity. *Journal of Cosmology and Astroparticle Physics*, 2019(06):020, 2019.
- [31] Lavrentios Kazantzidis and Leandros Perivolaropoulos. Evolution of the $f\sigma_8$ tension with the Planck15/ Λ CDM determination and implications for modified gravity theories. *Phys. Rev. D*, 97(10):103503, 2018.
- [32] Héctor Gil-Marín, Julien Guy, Pauline Zarrouk, Etienne Burtin, Chia-Hsun Chuang, Will J Percival, Ashley J Ross, Rossana Ruggeri, Rita Tojerio, Gong-Bo Zhao, et al. The clustering of the SDSS-IV extended Baryon Oscillation Spectroscopic Survey DR14 quasar sample: structure growth rate measurement from the anisotropic quasar power spectrum in the redshift range $0.8 < z < 2.2$. *Monthly Notices of the Royal Astronomical Society*, 477(2):1604–1638, 2018.
- [33] Jiamin Hou, Ariel G Sánchez, Román Scoccimarro, Salvador Salazar-Albornoz, Etienne Burtin, Héctor Gil-Marín, Will J Percival, Rossana Ruggeri, Pauline Zarrouk, Gong-Bo Zhao, et al. The clustering of the SDSS-IV extended Baryon Oscillation Spectroscopic Survey DR14 quasar sample: anisotropic clustering analysis in configuration space. *Monthly Notices of the Royal Astronomical Society*, 480(2):2521–2534, 2018.
- [34] N. Aghanim et al. Planck 2018 results. VI. Cosmological parameters. *Astron. Astrophys.*, 641:A6, 2020.
- [35] Dennis D Wackerly, Romo Muñoz, Jorge Humbertotr, et al. *Estadística matemática con aplicaciones*. Number 519.5 W3. 2010.
- [36] Eoin Ó Colgáin and M. M. Sheikh-Jabbari. Elucidating cosmological model dependence with H_0 . *Eur. Phys. J. C*, 81(10):892, 2021.
- [37] Marina Seikel and Chris Clarkson. Optimising Gaussian processes for reconstructing dark energy dynamics from supernovae. *arXiv preprint arXiv:1311.6678*, 2013.
- [38] John Salvatier, Thomas V Wiecki, and Christopher Fonnesbeck. Probabilistic programming in python using pymc3. *PeerJ Computer Science*, 2:e55, 2016.
- [39] Andrew Gelman and Donald B. Rubin. Inference from Iterative Simulation Using Multiple Sequences. *Statist. Sci.*, 7:457–472, 1992.
- [40] Ravin Kumar, Colin Carroll, Ari Hartikainen, and Osvaldo Martin. Arviz a unified library for exploratory analysis of bayesian models in python. *Journal of Open Source Software*, 4(33):1143, 2019.